

Superfluid-spiral state of quantum ferrimagnets in magnetic field

M. Abolfath^a, and A. Langari^{b,c}

^a *Department of Physics and Astronomy, University of Oklahoma, Norman, OK 73019-0225*

^b *Max-Planck-Institut für Physik komplexer Systeme, Nöthnitzer Strasse 38, D-01187 Dresden, Germany*

^c *Institute for Advanced Studies in Basic Sciences, Zanjan 45195-159, Iran*

(November 1, 2021)

We study the phase diagram of one-dimensional quantum ferrimagnets by using a numerical exact diagonalization of a finite size system along with a field-theoretical non-linear σ model of the quantum ferrimagnets at zero temperature and its effective description in the presence of the external magnetic field in terms of the quantum XY-model. The low- and the high-field phases correspond respectively to the classical Néel and the fully polarized ferromagnetic states where in the intermediate magnetic field ($h_{c1} < h < h_{c2}$), it is an XXZ+h model with easy plane anisotropy, which possess the spiral (superfluid) states that carry the dissipationless spin-supercurrent. We derive the critical exponents, and then will study the stability of the XY spiral state against these spin-supercurrents and the hard axis fluctuations. We will show a first order phase transition from the easy plane spiral state to a saturated ferromagnetic state occurs at $h = h_{c2}$ if the spin-supercurrent reaches to its critical value.

PACS number: 76.50.+g, 75.50.Gg, 75.10.Jm

I. INTRODUCTION

Recently, antiferromagnetically coupled mixed-spin chains with an alternating array of two kinds of spins have attracted interest among researchers [1–5]. Integrable models of mixed-spin antiferromagnetic chains were constructed by de Vega and Woynarovich [1] and the simplest case of such chains with spins $S = 1$ and $1/2$ were subsequently studied [2]. Since these integrable models are exactly solvable, they are very useful for studying (quantum) statistical mechanical properties. Although ferrimagnetic spin chains exhibit both ferromagnetic and antiferromagnetic features, they show some peculiar, and sometimes surprising, features uncharacteristic of either the ferromagnet or the antiferromagnet—an example being the existence of gapless excitations with very small correlation length. It is important to understand these features more clearly. In this paper we first present a numerical study on the quantum ferrimagnetic spin chain in magnetic field by an exact diagonalization of a finite size system. We show that the low- and the high-field phases correspond respectively to the classical Néel and the fully polarized ferromagnetic states where in the intermediate magnetic field ($h_{c1} < h < h_{c2}$), it is an XXZ+h model with easy plane anisotropy [4,5], and the critical exponents are derived numerically. Then the physical properties of the quantum ferrimagnets in the presence of the uniform magnetic field, as described by a phenomenological field theory based on a continuum non-linear σ model (NL σ M) formulation are examined further and will explore its novel features. When $h \geq h_{c1}$, the quantum ferrimagnets can be described by an easy-plane anisotropy state where the broken $U(1)$ symmetry of spins corresponds to a topological spiral (superfluid) state. A metastable state with a non-zero topological

spin-supercurrent J_s , is the superfluid state of the order parameter in XY-plane. Such possibility, may be led to the remarkable spin-dependent transport phenomenon in the ferrimagnetic chains, i.e., the spin-supercurrent is carried collectively (rather than by quasiparticles). Because the spin current is non-zero when the system is in equilibrium, it flows without dissipation. The spiral state can be characterized by a wave-vector Q , i.e., the soliton (saw tooth) lattice spacing $a = 2\pi/Q$ is a length scale through which the in-plane phase φ of the order parameter changes by 2π . Hence, the spin-supercurrent is characterized by these wave-vectors, e.g., $J_s \propto Q$. In analogy with the dissipation mechanism of the supercurrent in a one-dimensional superconductors [6], at large J_s , hard-axis fluctuations of the order parameter becomes unstable and a first order phase transition to a uniform in-plane state ($\varphi = \text{cte}$) takes place, and the long range order of the soliton lattice destroys. By overcoming the nucleation energy barrier of the order parameter vortices, a first order phase transition from easy plane spiral state to a saturated ferromagnetic state occurs at $h = h_{c2}$, depends on J_s , and Q . This transition turns out to a continuous cross-over if the initial state of the system at $h = h_{c1}$ holds the zero spin-supercurrent (a uniform easy plane with $Q = 0$). The possibility of the existence of the superfluid phase and crossing onto a saturated ferromagnetic state (the dependence of h_{c2} on Q , and J_s) are discussed in some detail.

The zero-temperature quantum ferrimagnetic chain is defined by $H = J \sum_{\langle ij \rangle} S_i \cdot s_j - h \sum_i (S_i + s_i)$ where $S \neq s$. The low energy physics of the quantum ferrimagnets in the presence of the external magnetic field can be obtained by a 1-dimensional NL σ M. The external magnetic field couples with \mathbf{n} , the Néel order parameter

$$\mathcal{L}_h = iM_0\mathbf{A}(\mathbf{n}) \cdot \partial_\tau \mathbf{n} + \mathcal{L}_{\text{NL}\sigma\text{M}+\text{h}} + \mathcal{L}_{\text{top}} - M_0\vec{h} \cdot \mathbf{n}, \quad (1)$$

where

$$\mathcal{L}_{\text{NL}\sigma\text{M}+\text{h}} = \frac{1}{2g} \left(v_s (\partial_x \mathbf{n})^2 + \frac{1}{v_s} [2i\vec{h} + \mathbf{n} \times \partial_\tau \mathbf{n}]^2 \right). \quad (2)$$

The first term in Eq. (1) is the usual (dynamical) Berry's phase of a quantum ferromagnet, with $M_0 \equiv |S - s|/a_0$ the magnetization per unit cell (pair of sites). Here \mathcal{L}_{top} is the topological term, $g = 4/(s + S)$, and $v_s = 4a_0JsS/(s + S)$ [5]. It is this term that results in the ferromagnetic branch of the spin waves and corresponds to the trajectory of spin over a closed orbit on the unit sphere in the presence of a unit magnetic monopole at the center. The contribution of the first term in \mathcal{L}_h is equivalent to the area enclosed by this trajectory and since either of the smaller or the larger enclosed areas on the unit sphere must lead to the same Berry's phase, the magnetic moment per unit cell, i.e. $2M_0a_0$, must be quantized with integral values [7]. Setting $M_0 = 0$ in action (1) follows to the usual $O(3)$ NL σ M in the magnetic field [8], applicable to the Heisenberg antiferromagnets. Similar to zero magnetic field [5] we can find the spin-wave modes. At $h = 0$ the ferrimagnetic spin-waves consist of both gapless (ferromagnetic) and gapped (antiferromagnetic) modes, and at $T = 0$ the low (high) energy physics of quantum ferrimagnets is effectively like that of a ferromagnet (antiferromagnet) which is formed by the chain of (dimerized) unit cells with magnetic moment $M_0 (= |S - s|)$. Applying an external magnetic field, h , develops a gapped ferromagnetic spin-waves; in which case the energy cost for the ferromagnetic transitions is proportional to the Zeeman splitting factor. Unlike to ferromagnetic mode, the effect of the external magnetic field is to suppress the antiferromagnetic gap. Clearly, this reveals similarities between the ferrimagnets and the integer spin Heisenberg antiferromagnets in magnetic field [9]. The ground state of the ferrimagnet corresponds to the *staggered* configuration of spins, unless $h \geq h_{c1} = 2J|S - s|$. At this point the staggered state becomes unstable against the non-collinear *spin-flop* phase (the partially polarized state) of the spins when the spectrum becomes soft at $k = 0$. When the external magnetic field exceeds h_{c2} , the system will be in a saturated ferromagnetic phase, with a quantized magnetization per unit cell. The $h_{c2} \equiv 2J(S + s)$ is obtained by using the dispersion relation of the spin waves based on the fully polarized state of the ferrimagnets. It is the lower-bound of the external magnetic field, in the sense that the spin waves of the fully polarized state become soft at $k = 0$.

The outline of this paper is as follows : In next section we will present the numerical computations of Lanczos method to compare the behavior of the correlation functions on the plateau and between two plateaux. We also derive the critical exponents, and the effective Hamiltonian for the latter region by using a Quantum Renormal-

ization Group (QRG) approach. The main part of this paper, the spiral (superfluid) state of the quantum ferrimagnets is presented in section III. The details of the collective modes in the intermediate magnetic phase is given as the appendix in Sec. IV.

II. NUMERICAL RESULTS

In order to have more accurate physical picture, we present the numerical results, by applying a Lanczos method to each S_z -sector of Hilbert space from $S_z = \frac{N}{2}(S - s)$ to $S_z = \frac{N}{2}(S + s)$. Here $N (= 20)$ is the number of sites that is used in the exact diagonalization.

A curve for magnetization vs. magnetic field for a chain of $(1/2, 1)$ -ferrimagnet has been given in Ref. [10]. An extrapolation to $N \rightarrow \infty$ on exact diagonalization calculation shows there are two plateaux of magnetization below $h_{c1} = \Delta_0 = 1.7589J$ and above $h_{c2} = 3J$, associated with the magnetization $m \equiv \frac{M}{S+s} = 1/3$ and $m = 1$. Here Δ_0 is the energy gap between the Ferro- and Antiferromagnetic spin wave modes of this model. In Fig. 1 the numerical results of the in-plane spin-spin correlations is presented for a point on the plateau (at $m = 1/3$) and some intermediate points between two plateaux, i.e., $m = 2/5, 8/15, 2/3$ and $4/5$. This exhibits the in-plane spin-spin correlation functions within the intermediate magnetic field region which falls off as power law, and manifests the critical behavior.

Thus the in-plane correlation is expected to have the asymptotic form $\langle S^x(0)S^x(r) \rangle \sim r^{-\eta}$. For instance we have calculated this exponent for $m=2/3$ by using data of exact diagonalization of a chain with length $N = 20$. Since there are correlations between different types of sublattices we find an exponent for each case. For correlations on sublattice A (Fig.1-(a)) and $m=2/3$ we obtained $\eta = 0.44 \pm 0.01$ and for sublattice B (Fig.1-(b)) we have $\eta = 0.42 \pm 0.04$. A similar behavior is seen for the correlations of different sublattices A and B (Fig.1-(c)) where $\eta = 0.47 \pm 0.01$. To have more qualitative picture of the transient region between two plateaux, we can use a quantum renormalization group. To perform this, we choose two adjacent spins ($S = 1, s = 1/2$) as the building block. The block Hamiltonian is then $H_B = J\mathbf{S} \cdot \mathbf{s} - h(S_z + s_z)$. For low field limit (e.g. $h < h_{c1}$) the lowest lying states of H_B are a spin-1/2 doublet. This comes out with an effective Hamiltonian of ferromagnetic Heisenberg chain with $S = 1/2$ in magnetic field, corresponds to the $m = 1/3$ plateau. For high field limit $h > 3J/2$ where two states $|S_T = 1/2, S_T^z = 1/2\rangle$, and $|S_T = 3/2, S_T^z = 3/2\rangle$ are nearly degenerate, we arrive with a spin-1/2 antiferromagnetic $XXZ + h$ Hamiltonian. The effective Hamiltonian is

$$H_{\text{eff}} = \frac{2J}{3} \sum_{n=1}^{N/2} (\tau_n^\perp \cdot \tau_{n+1}^\perp + \Delta \tau_n^z \tau_{n+1}^z) - h' \sum_{n=1}^{N/2} \tau_n^z \quad (3)$$

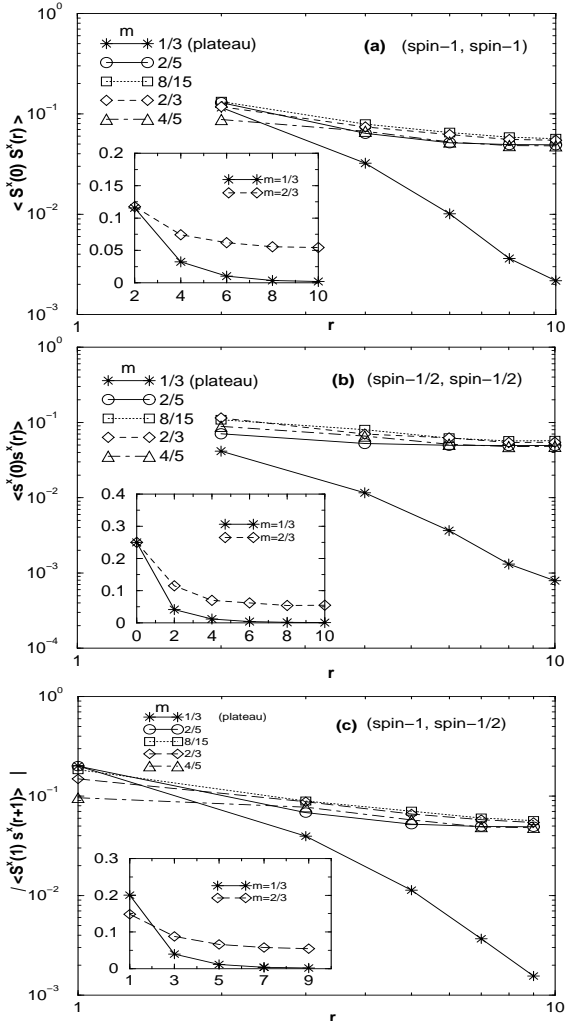


FIG. 1. The log-log plot of in-plane spin-spin correlation function is shown within the plateau ($m = 1/3$) and within the partially spin polarized state ($m = 2/5, 8/15, 2/3, 4/5$). The former shows the exponential decay while in the latter region the power law behavior of correlation function is seen. The correlation on sublattice A (spin-1, spin-1) is shown in (a), on sublattice B (spin-1/2, spin-1/2) in (b) and between the two sublattices A (spin-1) and B (spin-1/2) in (c). In (c) spin-1 is fixed and the position of spin-1/2 is running to show the correlations. In each part an inset represents the correlation for $m = 1/3$ and $2/3$ in a normal scale. The former approaches to zero exponentially, and the latter falls off algebraically.

where τ is spin-1/2 operator, $\Delta = 1/3, h' = \frac{3}{2}h - \frac{19}{6}J$. It is known such model Hamiltonian in the presence of a magnetic field (h) has a critical line which separates the partially polarized phase from the fully polarized one [11]. The magnetization of the ferrimagnetic chain (m) is related to the magnetization of $XXZ + h$ model by $m = 1 + m_{XXZ+h}$ which leads to the same behavior as the numerical results but with some discrepancies for the critical fields ($h_{c1} = 1.5J$, $h_{c2} = 3J$). However one may continue the quantum RG procedure for the $XXZ + h$ model and obtain that the RG flow for the par-

tially polarized phase (between the two plateaux) goes to the isotropic XY fixed point [12].

III. SUPERFLUID PHASE

By generalizing the $NL\sigma M+h$ we propose a phenomenological field theory which can present the long wave length limit of the quantum ferrimagnets within $h \geq h_{c1}$

$$E = \int dx \left[\frac{1}{2} \rho_s^\perp (\partial_x n_\perp)^2 + \frac{1}{2} \rho_s^z (\partial_x n_z)^2 + \beta n_z^2 - h^* n_z \right], \quad (4)$$

where we applied the spin coherent state formalism in Eq.(4). Here $h^* = h - h_{c1}$ is the effective magnetic field. ρ_s^\perp and ρ_s^z are in-plane and out of plane spin stiffness. $\beta > 0$ gives an easy plane anisotropy. To study a superfluid phase, it is convenient to introduce the following variational solutions $\mathbf{n}(x) = (\sin \theta \cos \varphi, \sin \theta \sin \varphi, \cos \theta)$, where $\theta = \theta(x)$ and $\varphi = Qx$. Here Q is a spiral state wave vector responsible for the superfluid phase slip, and $a = 2\pi/Q$ is the soliton lattice spacing, i.e., the phase φ changes by 2π along the chain. Clearly $\tilde{n}_z = \cos \theta$ is the uniform solution (θ is a constant) and $\tilde{E} = \rho_s^\perp Q^2 (1 - \tilde{n}_z^2)/2 + \beta \tilde{n}_z^2 - h^* \tilde{n}_z$ is the corresponding energy per unit length. Note n_z is the momentum density conjugate to field variable φ , and the Hamiltonian (4) gives a linearly dispersing collective mode, associated with the $U(1)$ symmetry breaking phase, i.e., the superfluid phase. It is easy to check how the classical solutions and the fluctuating modes can be derived by Eq.(4). For example $d\tilde{E}/d\tilde{n}_z = 0$ leads to $\tilde{n}_z = h^*/\tilde{K}_{zz}$ where $\tilde{K}_{zz} \equiv d^2\tilde{E}/d\tilde{n}_z^2 = 2\beta - \rho_s^\perp Q^2$ is the energy gap of the out-of-plane modes at zero wave vector. Then $J_s = (1/\hbar)d\tilde{E}/dQ = \tilde{n}_z^2 \rho_s^\perp Q/\hbar$ is the gauge invariance topological spin-supercurrent density carried along the x -direction. Furthermore, it is necessary to study the stability of the superfluid phase against the quantum fluctuations. This governs with the in-plane fluctuations $K_{\varphi\varphi}(k) = 2\rho_s^\perp \tilde{n}_z^2 k^2$, and the out of plane fluctuations

$$K_{zz}(k) = \rho_s^\perp \tilde{n}_z^2 (k^2 + Q^2) - \rho_s^\perp \tilde{n}_z^2 Q^2 + \rho_s^z \tilde{n}_z^2 k^2 + 2\beta(\tilde{n}_z^2 - \tilde{n}_z^2) + h^* \tilde{n}_z. \quad (5)$$

As one can see $\tilde{K}_{zz} = K_{zz}(k=0)$ at $h^* = 0$. The gapless linear superfluid mode can be obtained by $\hbar\omega = 2\sqrt{K_{\varphi\varphi}K_{zz}}$. The details of the collective modes calculation is presented in Appendix. Through out this formulation, the zero temperature phase diagram of this system can be obtained. At $h^* = 0$ where $\tilde{n}_z = 0$ the out of plane instability occurs at $Q_c = \sqrt{2\beta/\rho_s^\perp}$. At this point the energy gap of the zz -modes vanishes and the $O(3)$ symmetry of the Hamiltonian is restored (the dispersion relation of the collective modes become imaginary at small k). It

follows the transition to a uniform solution must occur at this point since $\pi_1(S^2) = 0$ where the linear solution can be considered as a map from the compactified physical space to the equator of the order parameter space S^2 . Such instability in order parameter space is induced by the local fluctuations of the order parameter, out of the equator toward the north pole of the order parameter space S^2 . When J_s is close to its critical values (J_{sc}), the local fluctuations are very strong, and it is likely the order parameter passes the north pole, and the phase φ becomes singular, i.e., a vortex is nucleated, and the phase winding is lost. The effect of h^* is pushing the spins to be aligned along z -axis, e.g., $\tilde{n}_z = 1$ at large enough h^* . We notice if $h > h_{c1}$, system undergoes onto the saturated ferromagnetic phase by increasing the spin-supercurrent density. This happens at $Q^* = \sqrt{(2\beta - h^*)/\rho_s^\perp} < Q_c$, corresponding to $J_s = 0$, before the outset of the easy-plane uniform state. To study the nucleating mechanism of the vortices, we implement a mechanical analogy to the classical field theory. This formalism has been developed by Langer, and Ambegaokar [6] for one dimensional superconductors. To avoid the complexity let us neglect ρ_s^z in energy functional (4) from now on. To start this calculation, we make the following transformations $n_x(x) = f(x) \cos \varphi(x)$, $n_y(x) = f(x) \sin \varphi(x)$, and $n_z(x) = \sqrt{1 - f^2(x)}$ (where $f \equiv n_\perp$), and

$$E[f] = \int dx \left(\frac{\rho_s^\perp}{2} \left[(\partial_x f)^2 + \frac{L^2}{f^2} \right] + \beta(1 - f^2) - h^* \sqrt{1 - f^2} \right), \quad (6)$$

where L is the momentum conjugate to φ and it is proportional to the spin-supercurrent density J_s , because $\partial_x \varphi = L/f^2$ is the solution of the $\delta E[f, \varphi]/\delta \varphi = 0$. It is straightforward to show how $\delta E[f]/\delta f = 0$ yields

$$x - x_0 = \int_{f(x_0)}^{f(x)} \frac{df}{2\sqrt{E_{\text{eff}} - U_{\text{eff}}(f)}}, \quad (7a)$$

$$\varphi(x) - \varphi(x_0) = L \int_{f(x_0)}^{f(x)} \frac{dx}{f^2}, \quad (7b)$$

$$-U_{\text{eff}}(f) = \frac{\rho_s^\perp L^2}{2f^2} + \beta(1 - f^2) - h^* \sqrt{1 - f^2}. \quad (7c)$$

Uniform solutions ($f = \tilde{f} = \text{cte}$) are one of the solutions of Eqs. (7). It leads to $\varphi = Qx$ and $L = Q\tilde{f}^2$. The energy potential associated with the uniform solutions are depicted in Fig. 2 where $-U_{\text{eff}}(f)$ vs. f is plotted for $h^* = J$ for different Q 's, or equivalently for different spin-supercurrent J_s . Here $\rho_s^\perp = 2J/3$, and $\beta = J$. The effective potential, $-U_{\text{eff}}$, has one minimum at $\tilde{f} = 1 - [h^*/(2\beta - \rho_s^\perp Q^2)]^2 \neq 0$ if $Q \leq Q^*$.

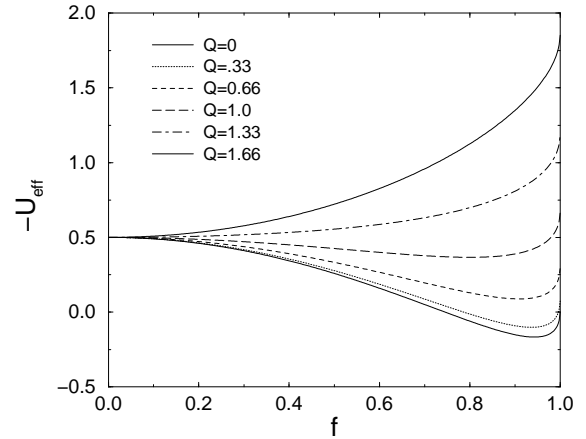


FIG. 2. $-U_{\text{eff}}(f)$, the effective potential of the spiral state vs. f is plotted for $h^* = J$. The minimum energy solution at $Q = Q^*$ is $f = 0$ where the spiral state destroys.

This minimum energy solution is disappeared if $Q > Q^* (= \sqrt{(2\beta - h^*)/\rho_s^\perp})$, and is replaced by another minimum at $\tilde{f} = 0$. At Q^* a first order phase transition from $\tilde{f} \neq 0$ onto $\tilde{f} = 0$ takes place by nucleating of a vortex. One can follow the transition between these minimum energy solutions by changing the parameters, Q and h^* , as illustrated in Fig. 2. The saddle point solutions can be derived by setting $d^2 U_{\text{eff}}/d\tilde{f}^2 = 0$ at the extremum of $U_{\text{eff}}(\tilde{f})$. It follows at $Q^* = \sqrt{(2\beta - h^*)/\rho_s^\perp}$ (or equivalently $J_s = 0$), the local minima at finite \tilde{f} is disappeared and $\tilde{n}_z = 1$ becomes a unique minima of U_{eff} . Moreover, the cross-over from the uniform state [a broken $U(1)$ symmetry state with zero spin-supercurrent] to a saturated ferromagnetic state occurs at $h^* = 2\beta = 2J$ ($Q^* = 0$), consistent with the exact diagonalization results ($h_{c2} = 3J$). Obviously at $h = h_{c1}$ and $Q = Q_c (= \sqrt{2\beta/\rho_s^\perp})$, the sign of curvature of $-U_{\text{eff}}$ changes, and therefore Q_c can be considered as the saddle point of $-U_{\text{eff}}$, at which the spiral state becomes unstable against the hard-axis fluctuations and a transition to a uniform solution occurs. This is seen if the spin-supercurrent J_s arrives to its critical value, J_{sc} . As was mentioned earlier, the mechanism for such transition is nucleating of a vortex in the order parameter space. For a given Q and h^* , it is straightforward to show $\tilde{E}(Q) = \rho_s^\perp Q^2/2 - h^{*2}/(2\beta - \rho_s^\perp Q^2)$. Recalling $J_s = (1/\hbar)d\tilde{E}(Q)/dQ$ leads to $J_s = \rho_s^\perp f^2 Q/\hbar$ ($J_s = \rho_s^\perp L/\hbar$) which is the spin-supercurrent density and $\tilde{n}_z = h^*/(2\beta - \rho_s^\perp Q^2)$ is the classical solution of Eq.(7). The dependence of $L (= Q[1 - h^{*2}/(2\beta - \rho_s^\perp Q^2)])$ with respect to Q for various h^* is illustrated in Fig. 3. It follows that J_s vanishes at $Q^* = \sqrt{(2\beta - h^*)/\rho_s^\perp}$ where the system crosses to the saturated ferromagnetic phase. The maximum spin-supercurrent $J_s^* (< J_{sc})$, which can pass through the system at finite wave vector Q (and

$h^* \neq 0$), is a monotonically decreasing function of h^* .

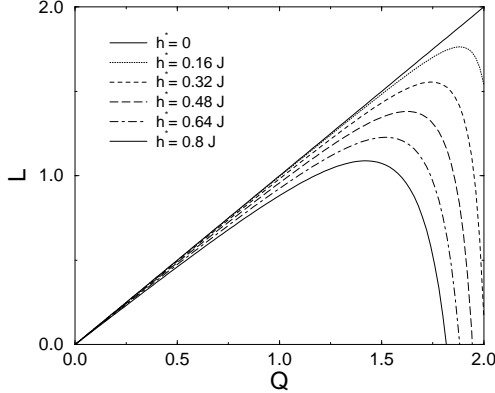


FIG. 3. L vs. Q is plotted for different h^* . For any h^* there is a maximum spin-supercurrent $J_s = J_s^* (< J_{sc})$ which can pass through the system at wave vector Q' . J_s^* is a monotonically decreasing function of h^* . At $Q = Q^* \neq 0$, the spin-supercurrent density vanishes ($L = 0$).

In conclusion, we have predicted the intermediate magnetic field region of ferrimagnets can support the dissipationless flow of the spin-supercurrents, which may be observed by the advance techniques of *spintronics*. The idea of the collective spin-supercurrent transport which has been presented in this paper is completely general, and can be applicable to any 1-dimensional spin system with easy plane anisotropy. The intermediate magnetic field phase of the ferrimagnets is one example. Other example of this kind is the *isospin*-supercurrent transport of the quantum Hall bars in the bilayer electron systems. [13]

IV. APPENDIX

Here we present the detailed calculation of the collective modes in the intermediate magnetic field phase. The effective Hamiltonian in terms of the in-plane and the out of plane fluctuations is given by

$$H_f[\varphi, n_z] = \frac{1}{2} \sum_q \varphi(-q) K_{\varphi\varphi}(q) \varphi(q) + \frac{1}{2} \sum_q n_z(-q) K_{zz}(q) n_z(q), \quad (8)$$

where $K_{\varphi\varphi} = \delta^2 E / \delta\varphi^2$ and $K_{zz} = \delta^2 E / \delta n_z^2$. The equation of motion for the field variables φ , and n_z can be obtained by the Hamilton equations ($\dot{p} = -\delta H / \delta q$ and $\dot{q} = \delta H / \delta p$)

$$\frac{dn_z(q)}{dt} = -\frac{\delta H_f}{\delta \frac{\hbar}{2} \varphi(-q)} = -\frac{2}{\hbar} K_{\varphi\varphi}(q) \varphi(q), \quad (9a)$$

$$\frac{d\varphi(q)}{dt} = \frac{\delta H_f}{\delta \frac{\hbar}{2} n_z(-q)} = \frac{2}{\hbar} K_{zz}(q) n_z(q), \quad (9b)$$

where n_z is the momentum density associated with the field variable φ . In the spin coherent representation, n_z and n_+ are given by $-i\hbar\partial/\partial\varphi$, and $e^{i\varphi}$ respectively. Then it is easy to check the transformation $n_z \rightarrow \partial_t\varphi$ can be obtained by canonical quantization, i.e., n_z can be considered as the momentum density conjugate to field variable φ . Making the derivative with respect to time we find the equation of motion: $\ddot{n}_z = -(2/\hbar)K_{\varphi\varphi}(q)\dot{\varphi}(q) = -(2/\hbar)^2 K_{\varphi\varphi}(q)K_{zz}(q)n_z$, where $\dot{\varphi} \equiv d\varphi/dt$. This clearly gives

$$\hbar\omega = 2\sqrt{K_{\varphi\varphi}(q)K_{zz}(q)}. \quad (10)$$

Eqs.(9a-9b) are similar to the coupled Josephson junction relations in superconductivity.

V. ACKNOWLEDGEMENT

We are grateful to Homayoun Hamidian who was involved in the early stage of this study. Useful conversation with Allan MacDonald, Miguel Martin-Delgado and Kieran Mullen is acknowledged. Work at the University of Oklahoma was supported by the NSF under grant No. EPS-9720651 and a grant from the Oklahoma State Regents for Higher Education.

-
- [1] H. J. de Vega and F. Woynarovich, J. Phys A **25**, 4499 (1992); H. J. de Vega, L. Mezincescu, and R. I. Nepomechie, Phys. Rev. B **49**, 13223 (1994).
 - [2] A. K. Kolezhuk, H.-J. Mikeska, and S. Yamamoto, Phys. Rev. B **55**, R3336 (1997); S. K. Pati, S. Ramasesha, and D. Sen, Phys. Rev. B **55**, 8894 (1997); S. Brehmer, H.-J. Mikeska, and S. Yamamoto, J. Phys.: Condens. Matter **9**, 3921 (1997); S. K. Pati, S. Ramasesha, and D. Sen, J. Phys. Condens. Matter **9**, 8707 (1997); G.-S. Tian, Phys. Rev. B **56**, 5355 (1997); S. Yamamoto and T. Fukuii, Phys. Rev. B **57** R14008 (1998); N. B. Ivanov, Phys. Rev. B **57** R14024 (1998); K. Maisinger, U. Schollwöck, S. Brehmer, H. J. Mikeska, and Shoji Yamamoto, Phys. Rev. B **58**, R5908 (1998).
 - [3] Shoji Yamamoto, S. Brehmer, H. J. Mikeska, Phys. Rev. B **57**, 13610 (1998).
 - [4] A. K. Kolezhuk, H.-J. Mikeska, K. Maisinger, and U. Schollwöck, Phys. Rev. B **59**, 13565 (1999).
 - [5] M. Abolfath, H. Hamidian, A. Langari, preprint cond-mat/9901063.

- [6] J. S. Langer, and Vinay Ambegaokar, Phys. Rev. **164**, 498 (1967).
- [7] N. Read, and S. Sachdev, Phys. Rev. Lett. **75**, 3509 (1995).
- [8] V. Nikos Nicopoulos, and A. M. Tsvelik, Phys. Rev. B **44**, 9385 (1991).
- [9] Tôru Sakai, and Minoru Takahashi, Phys. Rev. B **43** 13383 (1991).
- [10] The magnetization curve of a 1d ferrimagnets can be obtained by setting $\gamma = 1$ in the SBA configuration of two-leg ladder, presented in A. Langari and M. A. Martin-Delgado, Phys. Rev. B **62**, 11725 (2000), and normalizing the magnetic field by 2.
- [11] C.N. Yang and C. P. Yang, Phys. Rev. **150**, 321 (1966).
- [12] A. Langari, Phys. Rev. **B58**, 14467 (1998).
- [13] M. Abolfath, and Allan H. MacDonald (unpublished).